

Laws of Learning Dynamics and the Core of Learners

Inkee Jung ^{*1} Siu Cheong Lau ^{*1}

Abstract

We formulate the fundamental laws governing learning dynamics, namely the conservation law and the decrease of total entropy. Within this framework, we introduce an entropy-based lifelong ensemble learning method. We evaluate its effectiveness by constructing an immunization mechanism to defend against transfer-based adversarial attacks on the CIFAR-10 dataset. Compared with a naive ensemble formed by simply averaging models specialized on clean and adversarial samples, the resulting logifold achieves higher accuracy in most test cases, with particularly large gains under strong perturbations.

1. Introduction

In this paper, we develop a rigorous mathematical formulation of learning process of ensembles of models, and prove two fundamental laws governing learning dynamics: the conservation law and the decrease of entropy, which bear a strong formal resemblance to the First and Third Laws of Thermodynamics. Learning dynamics is a very rich and foundational subject, see for instance (Puterman, 1994; Anthony & Bartlett, 2009; Khalil, 2011; Bellman, 2010; Choromańska et al., 2014; Ge et al., 2015; Mandt et al., 2017; Mei et al., 2018; Soudry et al., 2018; Jacot et al., 2018). We will take a concise, mathematical and practical approach.

Entropy and cross entropy play crucial roles in machine learning and data science, providing a quantitative framework for measuring uncertainty and loss in predictive modeling, see for instance (Hendrycks & Gimpel, 2017; Guo et al., 2017; Depeweg et al., 2017). The concept of entropy has a long history, originating in 19th-century thermodynamics. The formulation most directly relevant to data science is Shannon entropy, introduced in his mathematical theory of communication (Shannon, 1948).

^{*}Equal contribution ¹Department of mathematics, Boston University, Boston, USA. Correspondence to: Inkee Jung <inkeej@bu.edu>, Siu Cheong Lau <sclouis@bu.edu>.

Preprint. February 6, 2026.

A model (Φ, f) for the truth function \mathcal{T} is defined as a composition of two functions: the Euclidean representation Φ that maps a part of the full domain to an Euclidean space (called a feature space), and the decision function f that maps the feature space to a subset of the truth labels. We study a modular AI architecture (Minsky, 1986; Andreas et al., 2016) in which an ensemble is composed of heterogeneous models acting on different input modalities and output subspaces. This puts modular ensembles, Mixture-of-Experts (Jacobs et al., 1991) and multimodal learning (Ngiam et al., 2011; Srivastava & Salakhutdinov, 2012; Baltrušaitis et al., 2019) into a unified framework, which have the advantages of reduced catastrophic forgetting (Goo), improved accuracy (Bengio et al., 2015; Shazeer et al., 2017; Lepikhin et al., 2020; Fedus et al., 2022; Radford et al., 2021), and finer control over training through targeted fine-tuning and model-level error attribution (Zoph et al., 2022).

The entropy of an ensemble, as formulated in this work, consists of two principal components: the total entropy over the union of the domains covered by the constituent models, and a measure of the complement of this union within the full domain of the underlying ground-truth function. This formulation reveals two fundamental ingredients of the learning process. The first is reinforcement and refinement (Williams, 1992; Sutton & Barto, 1998; Sutton et al., 1999; Mnih et al., 2015; Schulman et al., 2015; 2017; Haarnoja et al., 2018) within the union of domains already covered by existing models. The second is the expansion of the knowledge domain (Ben-David et al., 2010; Muandet et al., 2013; Ganin et al., 2016; Gulrajani & Lopez-Paz, 2020) through the training of new models on newly observed or generated data.

We implement this theory of learning process to locate untrustworthy predictions and to develop a defense mechanism against common types of adversarial attacks (Goodfellow et al., 2015; Carlini & Wagner, 2017; Tramer et al., 2020; Croce & Hein, 2020). The idea is to construct a logifold (Jung & Lau, 2024; 2025) that consists of two layers of models (also called generations). The first layer contains two types of models: those trained on original samples and those trained on weakly perturbed samples. The second layer consists of models trained on incoming (possibly strongly) perturbed samples detected by the first layer. We

use the total entropy of the first layer to identify perturbed samples which are then passed to the second layer. Beyond the static rejection or abstention mechanisms proposed in prior work (Laidlaw & Feizi, 2019; Pang et al., 2022; Chen et al., 2023), our system treats rejected samples as active signals to evolve into a newly immunized generation.

In this design, the first layer functions as an immunized system capable of detecting adversarial perturbations via entropy. Once a non-negligible volume of inputs is detected outside the core, the system transfers models from the first layer to a second layer, where additional training is performed using the detected adversarial samples. This hierarchical structure can be extended to multiple layers to strengthen defenses; however, in our experiments we restrict attention to a two-layer architecture. We evaluate the proposed approach on the CIFAR-10 (Krizhevsky, 2009) dataset under gradient-based attacks such as APGD and AutoAttack (Croce & Hein, 2020; Tramer et al., 2020). With immunization, our logifold achieves significantly higher accuracy than models trained solely on clean data, models trained solely on adversarially perturbed data, and a naive ensemble obtained by simply averaging all models.

2. Laws of Learning for a model

Let

$$\mathcal{T} : X \rightarrow Y$$

be a continuous measurable function that represents the truth where X is a topological measure space with $\mu(X) < +\infty$ and $1 < |Y| < \infty$. In other words, we assume that the actual world we want to model has no fuzziness.

Definition 2.1. A model (Φ, f) for the truth function \mathcal{T} is a continuous measurable map $\Phi : S \rightarrow \mathbb{R}^n$ for a measurable subset $S \subset X$ and a function

$$f = (f_1, \dots, f_t) : \mathbb{R}^n \rightarrow \Delta(T)$$

which is continuous on the image of Φ , and $\Delta(T)$ is the simplex of probability distributions on a finite subset $T \subset Y$ of t elements with $T \supset \mathcal{T}(S)$. Φ is called to be an Euclidean representation and f is called to be a decision function.

Definition 2.2 (Entropy of a model). Let

$$H : \Delta(T) \rightarrow \mathbb{R}_{\geq 0}, \quad H(y) = - \sum_{a=1}^t y_a \log_t y_a \quad (1)$$

be the Shannon entropy function. The total entropy of a model (Φ, f) for \mathcal{T} is

$$H(\Phi, f) := \int_S H(f_a(\Phi(x))) dx + \mu(X - \text{Dom}(\Phi)).$$

The second term comes from integration over $X - \text{Dom}(\Phi)$ of the maximal entropy value which is $\sum_{a=1}^t (-\frac{1}{|Y|} \log_{|Y|} \frac{1}{|Y|}) = 1$.

It is well-understood that the entropy quantifies the uncertainty of the model f . In other words,

Entropy is fuzziness.

Note that $H(\Phi, f)$ does not depend on the truth function \mathcal{T} : we do not need to know about \mathcal{T} in order to compute the entropy $H(\Phi, f)$.

Next, we consider the distance between f and the truth function \mathcal{T} which quantifies the error of the model f .

Definition 2.3 (Cross entropy between the truth and a model). Let

$$h : \Delta \times \Delta^\circ \rightarrow \mathbb{R}_{\geq 0}, \quad h(y, \gamma) = - \sum_{a=1}^d y_a \log \gamma_a$$

be the cross entropy function, where $\Delta = \{y \in \mathbb{R}_{\geq 0}^d : \sum_{a=1}^d y_a = 1\}$ and Δ° denotes its interior. The cross entropy between the truth function \mathcal{T} and a model (Φ, f) for \mathcal{T} is defined to be $H(\mathcal{T}, (\Phi, f)) = \int_S h(\mathcal{T}(x), f(\Phi(x))) dx + \mu(X - S)$, which equals

$$H(\mathcal{T}, (\Phi, f)) := \int_S -\log_t (f_{\mathcal{T}(x)}(\Phi(x))) dx + \mu(X - S)$$

where $f_y(s) := 0$ if $y \notin T$.

The second term comes from the integration over $X - S$ of the maximal cross entropy value $-\log_{|Y|} \frac{1}{|Y|} = 1$. The first term is $+\infty$ if the measure $\mu(\{x \in S : \mathcal{T}(x) \notin T\}) > 0$. We have avoided this by putting the requirement $\mathcal{T}(S) \subset T$ in Definition 2.1.

The difference between cross entropy and entropy is quantified by the following proposition. The left hand side is the total work done needed to go from (Φ, f) to \mathcal{T} against the gradient vector field of H that measures fuzziness. Interpreting the cross entropy $H(-, (\Phi, f))$ as potential, then the right hand side is the potential difference between \mathcal{T} and (Φ, f) . Thus, the identity is an analog of the **conservation law (The First Law of Thermodynamics)**:

Effort paid in learning the truth \mathcal{T} turns to potential.

Proposition 2.4 (Conservation Law of Learning).

$$\begin{aligned} & \int_{\text{Dom}(\Phi)} (\text{grad } H)|_{f(\Phi(x))} \cdot (\mathcal{T}(x) - f(\Phi(x))) dx \\ &= H(\mathcal{T}, (\Phi, f)) - H(\Phi, f). \end{aligned}$$

Proof. See Appendix A.1. □

Definition 2.5. A learning process of a model for \mathcal{T} is a sequence of models $(\Phi^{(i)}, f^{(i)})_{i=1}^N$ for $N \in \mathbb{Z}_{>1} \cup \{+\infty\}$ such that $\text{Dom}(\Phi^{(i)}) \subset \text{Dom}(\Phi^{(j)})$ and $H(\mathcal{T}, (\Phi^{(i)}, f^{(i)})) > H(\mathcal{T}, (\Phi^{(j)}, f^{(j)}))$ for $i < j$.

The **Law of Learning Dynamics** as:

Entropy decreases in a learning process.

This has interesting similarity with the Third Law of Thermodynamics for crystallization.

Theorem 2.6. Suppose that $(\Phi^{(i)}, f^{(i)})_{i=1}^{\infty}$ is a learning process such that $\lim_{i \rightarrow \infty} H(\mathcal{T}, (\Phi^{(i)}, f^{(i)})) = 0$. Then

$$\lim_{i \rightarrow \infty} H(\Phi^{(i)}, f^{(i)}) = 0.$$

In particular, there exists a learning subprocess $(\Phi^{(i_j)}, f^{(i_j)})_{j=1}^{\infty}$ such that the entropy decreases to zero.

Proof. First, note that both $-\log_{t_i} (f_{\mathcal{T}(x)}^{(i)}(\Phi^{(i)}(x)))$ and $-f^{(i)}(\Phi^{(i)}(x)) \log_{t_i} f^{(i)}(\Phi^{(i)}(x))$ are non-negative functions. By $\lim_{i \rightarrow \infty} H(\mathcal{T}, (\Phi^{(i)}, f^{(i)})) = 0$, for any $\epsilon, n > 0$, we can take i sufficiently large such that $\mu(X - \text{Dom}(\Phi^{(i)})) < \epsilon$ and

$$\int_{\text{Dom}(\Phi^{(i)})} -\log_{t_i} (f_{\mathcal{T}(x)}^{(i)}(\Phi^{(i)}(x))) < \frac{\epsilon}{n}$$

so that

$$\mu \left(\left\{ -\log_{t_i} (f_{\mathcal{T}(x)}^{(i)}(\Phi^{(i)}(x))) > \frac{1}{n} \right\} \right) < \epsilon.$$

We need to prove that the following quantity can be made arbitrary small:

$$\begin{aligned} & \int_{\text{Dom}(\Phi^{(i)})} \sum_{a=1}^{t_i} \left(-f_a^{(i)}(\Phi^{(i)}(x)) \log_{t_i} f_a^{(i)}(\Phi^{(i)}(x)) \right) dx \\ &= \int_{\text{Dom}(\Phi^{(i)})} \left(-f_{\mathcal{T}(x)}^{(i)}(\Phi^{(i)}(x)) \log_{t_i} f_{\mathcal{T}(x)}^{(i)}(\Phi^{(i)}(x)) \right) dx \\ &+ \int_{\text{Dom}(\Phi^{(i)})} \sum_{a \neq \mathcal{T}(x)} \left(-f_a^{(i)}(\Phi^{(i)}(x)) \log_{t_i} f_a^{(i)}(\Phi^{(i)}(x)) \right) dx. \end{aligned}$$

For the first term, we subdivide $\text{Dom}(\Phi^{(i)}) = A \cup B$ into two subsets according to whether $-\log_{t_i} f_{\mathcal{T}(x)}^{(i)}(\Phi^{(i)}(x)) \leq \frac{1}{n}$ or not. On A , the integrand $-f_{\mathcal{T}(x)}^{(i)}(\Phi^{(i)}(x)) \log_{t_i} f_{\mathcal{T}(x)}^{(i)}(\Phi^{(i)}(x)) \leq \frac{t_i^{-1/n}}{n} < \frac{1}{n}$, and hence the integral over A is less than $\frac{\mu(X)}{n} < \epsilon$ by taking n sufficiently large. On B , since $\mu(B) < \epsilon$ and the integrand $\leq \frac{1}{t_i}$, the integral is less than ϵ .

For the second term, we note that the set $C = \{x \in \text{Dom}(\Phi^{(i)}) : f_a^{(i)}(\Phi^{(i)}(x)) > 1 - t_i^{-1/n} \text{ for some } a \neq \mathcal{T}(x)\}$ is a subset of B which has measure $< \epsilon$. Since the integrand < 1 , the integral over C is less than ϵ . In the complement of C , the integrand $\leq -(t_i - 1)(1 - t_i^{-1/n}) \log_{t_i} (1 - t_i^{-1/n}) \leq -(|Y| - 1)(1 - |Y|^{-1/n}) \log_2 (1 - |Y|^{-1/n})$ which can be controlled to be $< \epsilon/\mu(X)$ by taking n large enough, so that the integral is less than ϵ . This finishes the proof. \square

$t_i^{-1/n}) \leq -(|Y| - 1)(1 - |Y|^{-1/n}) \log_2 (1 - |Y|^{-1/n})$ which can be controlled to be $< \epsilon/\mu(X)$ by taking n large enough, so that the integral is less than ϵ . This finishes the proof. \square

3. Law of Learning for an ensemble

Definition 3.1. An ensemble is a collection of models $\mathcal{U} = \{(\Phi_l, f_l) : l = 1, \dots, K\}$. Its knowledge domain is the union $\text{Dom}(\mathcal{U}) = \bigcup_{l=1}^K \text{Dom}(\Phi_l)$.

Definition 3.2 (Entropy for ensemble). For two models (Φ_1, f_1) and (Φ_2, f_2) , consider $F_i := f_i \circ \Phi_i : \text{Dom}(\Phi_1) \cap \text{Dom}(\Phi_2) \rightarrow \Delta(T_1 \cup T_2)$. The cross entropy over their common intersection is defined to be $H((\Phi_1, f_1), (\Phi_2, f_2)) := \int_{\text{Dom}(\Phi_1) \cap \text{Dom}(\Phi_2)} h(F_1(x), F_2(x)) dx$.

For an ensemble of models $\mathcal{U} = \{(\Phi_l, f_l) : l = 1, \dots, K\}$, the pointwise entropy of \mathcal{U} at $x \in X$ is defined as

$$H_x(\mathcal{U}) = \frac{1}{K_x^2} \sum_{\substack{l: \text{Dom}(\Phi_l) \ni x \\ r: \text{Dom}(\Phi_r) \ni x}} h(F_l(x), F_r(x)) \quad (2)$$

if $x \in \text{Dom}(\mathcal{U})$ and $K_x > 0$ is the number of models with $\text{Dom}(\Phi_l) \ni x$; otherwise $H_x(\mathcal{U})$ is

$$\frac{1}{K^2} \sum_{l,r=1}^K \sum_{a=1}^{|Y|} -\frac{1}{|Y|} \log_{|Y|} \frac{1}{|Y|} = 1.$$

The total entropy is defined to be

$$H(\mathcal{U}) = \int_X H_x(\mathcal{U}) = \int_{\text{Dom}(\mathcal{U})} H_x(\mathcal{U}) + \mu(X - \text{Dom}(\mathcal{U})). \quad (3)$$

For two ensembles of models $\mathcal{U} = \{(\Phi_l, f_l) : l = 1, \dots, L\}$, $\mathcal{V} = \{(\Psi_r, g_r) : r = 1, \dots, R\}$, the pointwise cross entropy of $(\mathcal{U}, \mathcal{V})$ at $x \in X$ is defined as

$$H_x(\mathcal{U}, \mathcal{V}) = \frac{1}{L_x R_x} \sum_{\substack{l: \text{Dom}(\Phi_l) \ni x \\ r: \text{Dom}(\Psi_r) \ni x}} h((f_l \circ \Phi_l)(x), (g_r \circ \Psi_r)(x)) \quad (4)$$

if $L_x > 0$ and $R_x > 0$ where $L_x = |\{l : \text{Dom}(\Phi_l) \ni x\}|$ and $R_x = |\{r : \text{Dom}(\Psi_r) \ni x\}|$;

$$\frac{-1}{R_x |Y|} \sum_{r: \text{Dom}(\Psi_r) \ni x} \log_{t_r} \prod_{a=1}^{t_r} (g_{r,a} \circ \Psi_r)(x)$$

if $L_x = 0$ and $R_x > 0$, and

$$\frac{-1}{L_x} \sum_{l: \text{Dom}(\Phi_l) \ni x} \sum_a F_{l,a} \log_{|Y|} \frac{1}{|Y|} = 1$$

otherwise. The total cross entropy $H(\mathcal{U}, \mathcal{V})$ is the integration of $H_x(\mathcal{U}, \mathcal{V})$ over X .

In particular, the pointwise cross entropy of the truth function \mathcal{T} and \mathcal{U} is the average cross entropy:

$$H_x(\mathcal{T}, \mathcal{U}) = \frac{1}{L_x} \sum_{l: \text{Dom}(\Phi_l) \ni x} h(\mathcal{T}(x), (f_l \circ \Phi_l)(x)) \quad (5)$$

if $x \in \text{Dom}(\mathcal{U})$ and 1 otherwise.

Remark 3.3. We can also consider the entropy $H(\bar{F})$ of the average function \bar{F} of $\{(\Phi_i, f_i)\}_{i=1}^K$, which is defined by $\bar{F}(x) = \frac{1}{L} \sum_{l: \text{Dom}(\Phi_l) \ni x} f_i(\Phi_i(x))$ if $L := |\{l : \text{Dom}(\Phi_l) \ni x\}| > 0$ and $\bar{F}_a(x) = 1/|Y|$ for all a otherwise. This is different from the entropy of the ensemble $H(\mathcal{U})$ defined above and loses information about disagreements of models in the ensemble. For instance, suppose \mathcal{U} consists of two model functions F_1, F_2 with $F_1(x_1) = (0.6, 0.4), F_2(x_1) = (0.6, 0.4)$ at x_1 , and $F_1(x_2) = (0.95, 0.05), F_2(x_2) = (0.25, 0.75)$ at x_2 . At the two points, the average is the same, $\bar{F}(x_1) = \bar{F}(x_2) = (0.6, 0.4)$, and hence $H_{x_1}(\bar{F}) = H_{x_2}(\bar{F})$. On the other hand, since F_1 and F_2 have big disagreement at x_2 , $H_{x_2}(\mathcal{U}) > H_{x_1}(\mathcal{U})$.

Remark 3.4. For a broad information-theoretic analysis of predictive-uncertainty measures, including cross-entropy based formulations, we refer the reader to (Schweighofer et al., 2025).

$H(\mathcal{U})$ is the degree of fuzziness of the ensemble of models \mathcal{U} . In particular,

Theorem 3.5 (Vanishing of entropy). *For an ensemble of models $\mathcal{U} = \{(\Phi_l, f_l) : l = 1, \dots, K\}$,*

$$H(\mathcal{U}) = 0$$

if and only if the models cover the whole space in measure sense, that is $X - \bigcup_{l=1}^K \text{Dom}(\Phi_l)$ has measure zero, and there exists a function $F : X \rightarrow Y$ such that for every $l = 1, \dots, K$, $F|_{\text{Dom}(\Phi_l)} = f_l \circ \Phi_l$ almost everywhere.

Proof. See Appendix A.2. \square

When each model in the ensemble is given by a fuzzy linear logical function (which gives a mathematical interpretation of a neural network), this is called to be a **fuzzy linear logifold**, see Definition 9 of (Jung & Lau, 2025). A strict linear logifold is given by Definition 8 of (Jung & Lau, 2025). The terminology of a logifold is motivated from manifold theory in which the space is covered by charts of observers. For a manifold, different charts are required to agree with each other and are glued together over overlapping regions; in contrast, fuzziness and disagreement among charts are allowed for a fuzzy logifold and are measured by entropy. By the above theorem,

Corollary 3.6. *A fuzzy linear logifold is a strict linear logifold if and only if its entropy vanishes.*

Definition 3.7. Given $0 < p < \min\{\frac{2}{|Y|}, \log_{|Y|} \frac{3}{2}\}$, the core of an ensemble of models $\mathcal{U} = \{(\Phi_l, f_l) : l = 1, \dots, K\}$ in threshold p is defined to be the subset

$$C_p(\mathcal{U}) = \{x \in X : H_x(\mathcal{U}) < p\} \subset X$$

where $H_x(\mathcal{U})$ is the pointwise entropy in Definition 3.2.

Proposition 3.8 (Non-fuzzy limit of the core). *In the core $C_p(\mathcal{U})$ of an ensemble $\mathcal{U} = \{(\Phi_l, f_l) : l = 1, \dots, K\}$ where $0 < p < \min\{\frac{2}{|Y|}, \log_{|Y|} \frac{3}{2}\}$, for every $x \in C_p(\mathcal{U})$ and l such that $\text{Dom}(\Phi_l) \ni x$, there exists a unique $a = a_{l,x} \in T_l$ that $f_{l,a} \circ \Phi_l(x) \in [0, 1]$ achieves maximum; moreover, $a_{l,x}$ are the same for all such l . Thus, this defines a function*

$$F : C_p(\mathcal{U}) \rightarrow Y$$

which is called to be the non-fuzzy limit of the ensemble restricted to the core.

Proof. See Appendix A.3. \square

Below is an analog of Proposition 2.4 for ensemble learning. The proof is similar and is omitted. The left hand side is the work done to go from the average of the ensemble to the truth \mathcal{T} against the average gradient vectors of H that measures fuzziness. This turns to the potential energy defined by the cross entropy $H(-, \mathcal{U})$.

Proposition 3.9 (Conservation law of ensemble learning).

$$\int_{\text{Dom}(\mathcal{U})} V(x) \cdot (\mathcal{T}(x) - f(x)) dx = H(\mathcal{T}, \mathcal{U}) - H(\mathcal{U}) \quad (6)$$

where

$$f(x) = \frac{1}{L_x} \sum_{l: \text{Dom}(\Phi_l) \ni x} f_l(\Phi_l(x)) \quad (7)$$

and

$$V(x) = \frac{1}{L_x} \sum_{l: \text{Dom}(\Phi_l) \ni x} (\text{grad } H)|_{f_l(\Phi_l(x))} \quad (8)$$

denote the average of models and the average of gradient vectors respectively.

Definition 3.10 (Learning process of an ensemble). A learning process of an ensemble of models for \mathcal{T} is a sequence of ensembles $(\mathcal{U}^{(i)})_{i=1}^N$ and injective functions

$$\mathcal{L} : \mathcal{U}^{(i)} \rightarrow \mathcal{U}^{(i+1)}$$

for $i = 1, \dots, N-1$ such that $\text{Dom}(\mathcal{U}^{(i)}) \subset \text{Dom}(\mathcal{U}^{(j)})$ and $H(\mathcal{T}, \mathcal{U}^{(i)}) > H(\mathcal{T}, \mathcal{U}^{(j)})$ for $i < j$, with the additional assumption that if $N = \infty$, the domain and the

target of each model stabilizes: for each i and each element $\Phi \in \mathcal{U}^{(i)}$, there exists k such that $\text{Dom}(\mathcal{L}^j(\Phi)) = \text{Dom}(\mathcal{L}^{j+1}(\Phi))$ and $T(\mathcal{L}^j(\Phi)) = T(\mathcal{L}^{j+1}(\Phi))$ for all $j \geq k$. The models in $\mathcal{U}^{(i+1)}$ that are not in the image of \mathcal{L}_i are said to be created in the i -th step; the models $\Phi \in \mathcal{U}^{(i+1)}$ with $\text{Dom}(\Phi) = \emptyset$ are said to be annihilated in the i -th step.

We have the following **Law of Learning Dynamics for ensemble**:

Theorem 3.11. *Let $(\mathcal{U}^{(i)})_{i=1}^{\infty}$ be a learning process of an ensemble of models for \mathcal{T} such that $\lim_{i \rightarrow \infty} H(\mathcal{T}, \mathcal{U}^{(i)}) = 0$. Then*

$$\lim_{i \rightarrow \infty} H(\mathcal{U}^{(i)}) = 0.$$

In particular, there exists a learning subprocess $(\mathcal{U}^{(i_j)})_{j=1}^{\infty}$ such that the entropy $H(\mathcal{U}^{(i_j)})$ decreases to zero.

Proof. See Appendix A.4. \square

4. Entropy-based lifelong ensemble learning

Lifelong learning addresses situations where a learner faces a stream of learning tasks, providing an opportunity for knowledge transfer across tasks (Thrun, 1998; Kirkpatrick et al., 2017; Guo et al., 2019; Parisi et al., 2019).

In the context of the learning process in Definition 3.10, the sequence of tasks is to learn the truth function on an expanding subsets of the domain over time. We consider a sequence of multiple learners where the earlier learners retain the memory of previous tasks, and new learners are created and transferred to new tasks. Earlier learners decide whether to pass a given task to the next generation by the entropy which measures uncertainty and disagreement among them. This multi-generational approach complements standard Deep Ensembles (Lakshminarayanan et al., 2017; Ovadia et al., 2019), which can be fragile on outlier predictions. Concretely, this is determined by entropy thresholds and the core in Definition 3.7; the earlier learners are annihilated if their core becomes an empty set.

Definition 4.1 (Lifelong learning). Let E be a set whose elements are called environments, A be a set whose elements are called actions, and $\mathcal{X}_e = (\mathcal{X}, \mu_e)$ where \mathcal{X} is a topological space called the data space with a probability measure μ_e that depends on environments $e \in E$. A learner is a tuple (K, U, π) where K is a topological space called the knowledge state space, $U : K \times \mathcal{X} \rightarrow K$ is called the learning rule, and $\pi : K \times E \rightarrow A$ is called the performance policy. Let $P : A \times E \rightarrow \mathbb{R}$ that evaluates actions in different environments and $I : A \rightarrow \mathbb{R}$ that measures memory formation.

A lifelong learning process is an infinite sequence $(e_i, x_i, k_i) \in E \times \mathcal{X} \times K$, where x_i are drawn accord-

ing to the measure μ_{e_i} and k_i is determined by $k_i = U(k_{i-1}, x_{i-1})$ and the initial k_0 such that the evaluation and memory formation are non-decreasing up to a prefixed $\epsilon > 0$:

$$\begin{aligned} P(\pi(k_{i+1}, e_{i+1}), e_{i+1}) &> P(\pi(k_i, e_{i+1}), e_{i+1}) - \epsilon; \\ I(\pi(k_{i+1}, e_{i+1})) &> I(\pi(k_i, e_{i+1})) - \epsilon. \end{aligned}$$

In a classification task, \mathcal{X} is the product $X \times Y$ of the input space and the labeling set. In practice, \mathcal{X}_e is replaced by its own product \mathcal{X}_e^N for some N , meaning that we take a batch of training and validation samples according to the measure μ_e rather than a single sample in each learning step. For a neural network model, K is the parameter space of the model, E is the set of all possible testing batches and A is the set of all possible predictions (in the form of probability distributions on the labeling set) for the input testing batches. P measures the accuracy and I measures the entropy.

However, if the environment changes rapidly and drastically over time, catastrophic forgetting may happen (McCloskey & Cohen, 1989; van de Ven et al., 2025) which crashes lifelong learning, namely the inequality for I is violated. For this purpose, we consider an ensemble of learners instead to better retain memory. See also Nested Learning recently introduced in (Goo).

Definition 4.2 (Lifelong ensemble learning). Let E, A, \mathcal{X}_e, P be the environment set, the action set, the data space and the evaluation of actions as before. Moreover, I is given as a function $A^n \rightarrow \mathbb{R}$ that measures overall memory formation for an arbitrary number n of learners. Given an infinite sequence of environments $e_i \in E \times \mathcal{X}$ which produce samples $x_i \in \mathcal{X}_{e_i}$, a lifelong ensemble learning process is an infinite sequence

$$(\mathcal{U}^{(i)}, \Gamma^{(i)}, (k_l^{(i)} : l \in \mathcal{U}^{(i)}))_{i=1}^{\infty}$$

where each $\mathcal{U}^{(i)}$ is an ensemble of finitely many learners, $\Gamma^{(i)} : A^{|\mathcal{U}^{(i)}|} \rightarrow A$ is the aggregation of individual actions (voting), with injective functions $\mathcal{L}^{(i)} : \mathcal{U}^{(i)} \rightarrow \mathcal{U}^{(i+1)}$ where $l \in \mathcal{U}^{(i)}$ and $\mathcal{L}^{(i)}(l)$ are the same learner (meaning (K, U, π) remains the same), and individual knowledge states $k_l^{(i)} \in K_l^{(i)}$ are updated according to $U_l^{(i)}$ as before. The evaluation P and memory formation I for the aggregated action $\Gamma^{(i)}((\pi_l^{(i)}(k_l^{(i)}, e_i) : l \in \mathcal{U}^{(i)}))$ are required to satisfy the same inequalities as before.

The idea is to use entropy thresholds set by accuracy evaluated on validation samples to decide the aggregation policy $\Gamma^{(i)}$. This suggests the following procedure for a classification task.

1. We start with a subset of the domain $S^{(1)} \subset X$. Using the data $\{(x, \mathcal{T}(x)) : x \in S^{(1)}\}$ (which is partitioned into training and validation subsets), we train

and validate an ensemble of models $\mathcal{U}^{(1)}$ whose domains are subsets of $S^{(1)}$ that cover $S^{(1)}$ and whose targets are subsets of $\mathcal{T}(S^{(1)})$. The entropy in Definition 3.2 is measured with respect to $S^{(1)}$. (At this stage, $\mu(X - S^{(1)})$ is dropped since it is unknown and cannot be measured).

2. For a preset high accuracy threshold, we use the validation data to find a low enough entropy threshold p such that on the core $C_p(\mathcal{U}^{(1)})$ of Definition 3.7, the ensemble $\mathcal{U}^{(1)}$ reaches the required accuracy on the validation data. We restrict the domain of $\mathcal{U}^{(1)}$ to be $C_p(\mathcal{U}^{(1)})$, and train the next generation of models $\mathcal{U}^{(2)'}$ whose domain is restricted to be $S^{(1)} - C_p(\mathcal{U}^{(1)})$. Then we take $\mathcal{U}^{(2)} = \mathcal{U}^{(1)} \cup \mathcal{U}^{(2)'}$. Note that the entropy threshold p could be zero, in which case the required accuracy threshold could not be reached and the first generation $\mathcal{U}^{(1)}$ is annihilated.
3. The above process can be repeated several times until the overall accuracy reaches a satisfactory level. If necessary, we may enlarge the models in the next generation to reach higher accuracy.
4. Next, we enlarge the domain subset $S^{(1)}$ to $S^{(2)} \subset X$ by finding more samples from the real world or generating more samples by different means such as adding random noises, acting by symmetries, or adversarial attacks. The entropy in Definition 3.2 is updated over the bigger subset $S^{(2)}$ accordingly. The entropy thresholds in each layer of the ensembles are recalculated to match the required accuracy threshold. More generations of models are created as before and some earlier generations are annihilated, until the overall accuracy reaches a satisfactory level.
5. The above procedure is repeated until the domain X is saturated by training and validation samples.

5. Immunized systems against adversarial attacks

We empirically support the proposed learning dynamics on the CIFAR-10 dataset. We construct a system that consists of generations of neural network models, where the domain of each generation is restricted according to the entropies of generations. More precisely, the domain of the first generation is restricted to its core (Definition 3.7); the domain of the second generation is restricted to the intersection of its core with the out-core (the complement of the core) of the first generation; and the domain of the last generation is restricted to the complement of all restricted domains of the previous generation. Such an ensemble of neural network models with restricted domains is called a logifold in (Jung & Lau, 2024; 2025). This perspective is closely related to

selective classification with an abstain/reject option, where uncertain or unsafe inputs are rejected rather than force-classified (Laidlaw & Feizi, 2019; Wang & Yiu, 2021; Chen et al., 2023).

Distance-based detectors can be sensitive to preprocessing and other sources of mismatch (Lee et al., 2018). We will use *ensemble entropy to detect the change of environments in lifelong learning*. Namely, when an unusual amount of inputs lie outside the core of the logifold, the system determines that the environment has changed and it initiates an adaptation procedure, which resets the entropy thresholds of the generations to reach a satisfactory accuracy for the training samples in the new environment, possibly annihilates some of the early generations if their thresholds are almost zero, and transfers models in the early generations to form a new generation to learn the samples that are out of core.

In this paper, we use adversarial perturbations primarily as a controlled mechanism to expand the observed domain and to stress test the stability of the logifold. First, we start with the clean environment e_0 , where we have a distribution supported over clean samples and train an ensemble of models $\mathcal{U}^{(0)}$ on these clean samples. Then we raise a white-box adversarial attack on $\mathcal{U}^{(0)}$. In the experiment to be described in the next section (see Table 1), we find that the core of $\mathcal{U}^{(0)}$ can detect the attacks without the knowledge of accuracy rate. Thus, an environmental change from e_0 to e_1 is detected, and some of the models are transferred to e_1 and added to $\mathcal{U}^{(0)}$ to form a new ensemble $\mathcal{U}^{(1)}$.

We will see that the core of $\mathcal{U}^{(1)}$ detects white-box strong adversarial attacks against itself even better than that of $\mathcal{U}^{(0)}$. For this, we take an even stronger white-box adversarial attacks (in terms of the size of perturbations and the number of steps) against $\mathcal{U}^{(1)}$. Compared to the same degree of attacks to $\mathcal{U}^{(0)}$, the core coverage of $\mathcal{U}^{(1)}$ exhibits a more significant drop and the core accuracy of $\mathcal{U}^{(1)}$ is higher. We call this to be an **immunization effect**, and call $\mathcal{U}^{(1)}$ to be an immunized generation whose core is more sensitive to adversarial environments.

Then the immunization mechanism works as follows. When a non-negligible volume of incoming samples lie outside the core of $\mathcal{U}^{(1)}$, the system determines that it is under a strong adversarial environment. Then it adds the second generation $\mathcal{U}^{(2)'}$ consisting of models that are trained on union of the strong adversarial and original samples that lie outside the core of $\mathcal{U}^{(1)}$. The final immunized system $\mathcal{U}^{(2)}$ (which is also denoted as IMM) consists of both generations $\mathcal{U}^{(1)}$ and $\mathcal{U}^{(2)'}$. In the testing/application stage, testing samples that lie in the core of $\mathcal{U}^{(1)}$ are processed by $\mathcal{U}^{(1)}$, and those that lie outside the core of $\mathcal{U}^{(1)}$ are processed by $\mathcal{U}^{(2)'}$. Comparing to a simple average of all models, this mechanism gains a higher accuracy on the whole union of samples, see Table 2a.

Note that we are not claiming for theoretical robustness concerning worst-case guarantees over all small perturbations of data points, which requires the knowledge of almost all data points and has a trade-off with accuracy (Tsipras et al., 2018; Zhang et al., 2019). In (Bai et al., 2024), accurate models are mixed with robust models to alleviate the accuracy-robustness trade-off. In our design, in addition to taking average of an ensemble, we aim at detecting effective attacks on $\mathcal{U}^{(1)}$ by using the entropy of $\mathcal{U}^{(1)}$, and maximizing the accuracy on the union of the original and adversarial samples by the use of entropy of the multi-generation design.

5.1. Experimental setup

We use the standard CIFAR-10 split (50,000 train / 10,000 test) and an ensemble of $K = 8$ independently trained classifiers: four VGG-type (Liu & Deng, 2015) and four ResNet-type (He et al., 2015) networks. The baseline ensemble predictor \bar{f} is the probability average.

We evaluate on clean data and on adversarial counterparts generated from the same splits, as well as their union

$$\mathcal{D}_{\text{union}} := \mathcal{D}_{\text{clean}} \cup \mathcal{D}_{\text{weak}} \cup \mathcal{D}_{\text{strong}}.$$

All adversarial examples are ℓ_2 -bounded and clipped to $[0, 1]$. We run untargeted ℓ_2 APGD-CE (Tramer et al., 2020) against \bar{f} with configurations

$$(\epsilon, \epsilon_{\text{step}}, \text{steps}, \text{restarts}) \in \{(0.5, 0.2, 2, 4), (0.7, 0.2, 10, 4)\},$$

denoted as APGD-weak ($\mathcal{D}_{\text{weak}}$) and APGD-strong ($\mathcal{D}_{\text{strong}}$), respectively. We also generate transfer-based adversarial examples using AutoAttack (Croce & Hein, 2020) with surrogate models from RobustBench (Croce et al., 2021); we use the CIFAR-10 Standard ℓ_2 surrogate and run AutoAttack at $\epsilon = 0.5$.

We replace the integrals in Equation (3) for total entropy H by empirical averages over the evaluation set, and drop the complement term as in Definition 4.2.

5.2. Specialization, composing generations, and evaluation

In the logfold viewpoint, each model acts as a chart whose effective domain and decision boundary may differ across charts. Rather than training a new network per chart, we reuse the penultimate feature backbone and adapt only the classification head.

Specialization. Given a trained classifier and a dataset, we replace the final dense+softmax head and fine-tune with Adam (Kingma & Ba, 2015) and categorical cross-entropy for 21 epochs using a stepwise learning-rate schedule.

Table 1. Core coverage and core accuracy under white-box ℓ_2 APGD-CE attacks (weak/strong configurations) at entropy threshold $\tau = 0.95$, which is selected for $\mathcal{U}^{(0)}$ to have greater than 90% core coverage on clean sample. We report single models (ResNet/VGG), the baseline ensemble $\mathcal{U}^{(0)}$, specialists (SPs), and the immunized generation $\mathcal{U}^{(1)}$. Under strong attacks, single models fail to detect perturbed samples in terms of core coverage. $\mathcal{U}^{(1)}$ yields the smallest core and the highest core accuracy among the three ensembles, which best distinguishes the effective adversarial samples among these cases.

| | | Clean | APGD-CE Weak | APGD-CE strong |
|---------------------|----------|----------------------|----------------------|----------------------|
| ResNets | Cov. (%) | 100 | 100 | 100 |
| | Acc. (%) | 91.35 (± 0.67) | 20.75 (± 4.04) | 17.43 (± 4.07) |
| VGGs | Cov. (%) | 100 | 100 | 100 |
| | Acc. (%) | 91.38 (± 0.82) | 52.54 (± 3.56) | 46.97 (± 4.94) |
| $\mathcal{U}^{(0)}$ | Cov. (%) | 90.50 | 72.96 | 51.07 |
| | Acc. (%) | 97.26 | 88.50 | 22.62 |
| SPs | Cov. (%) | 94.02 | 83.77 | 49.48 |
| | Acc. (%) | 93.70 | 88.70 | 32.32 |
| $\mathcal{U}^{(1)}$ | Cov. (%) | 89.38 | 75.08 | 43.06 |
| | Acc. (%) | 97.39 | 94.21 | 34.58 |

Compute environment. Experiments were run on the BU SCC cluster using an NVIDIA L40S GPU.

5.3. Results

Ensemble entropy versus single-model entropy. We evaluate core coverage and core accuracy under white-box ℓ_2 APGD-CE (weak/strong) at a fixed entropy threshold $\tau = 0.1$. For a single model, entropy thresholding does not produce a reliable core under adversarial perturbations: many misclassified adversarial samples still receive high confidence, yielding small H_x while core accuracy remains low.

Let $\mathcal{U}^{(0)}$ be the baseline ensemble (four VGG-type and four ResNet-type models trained on clean data). Under a white-box attack on \bar{f} , the core of $\mathcal{U}^{(0)}$ shrinks substantially on adversarial inputs. This shows that ensemble entropy of Definition 3.2 behaves better than the entropy of the average of $\mathcal{U}^{(0)}$ treated as a single model (see Remark 3.3) for this purpose.

We then add four ResNet specialists trained on APGD-weak samples generated against $\mathcal{U}^{(0)}$. Let SPs denote these models and define $\mathcal{U}^{(1)} = \mathcal{U}^{(0)} \cup \text{SPs}$ ($K_1 = 12$), which we call the immunized generation. Table 1 reports that $\mathcal{U}^{(1)}$ yields a smaller core and higher core accuracy than $\mathcal{U}^{(0)}$ and SPs under strong attacks.

Evaluation across environments and memory formation. We run lifelong ensemble learning over $\mathcal{D}_{\text{clean}}$, $\mathcal{D}_{\text{weak}}$, $\mathcal{D}_{\text{strong}}$, and $\mathcal{D}_{\text{union}}$, where “weak”/“strong” refer to adversarial samples generated against $\mathcal{U}^{(0)}$. For each domain, we select an entropy threshold τ on a valida-

Table 2. Overall accuracy and total entropy at entropy thresholds τ selected on validation data to ensure high first-generation core accuracy. $\mathcal{U}^{(0)}$: 8 scratch-trained models. $\mathcal{U}^{(1)}$: 12-model immunized generation. IMM = $\mathcal{U}^{(1)} \cup \mathcal{U}^{(2)'}'$ with four out-of-core specialists. “All-ens” averages all members in IMM.

(a) Overall accuracy on each domain at the selected τ . Except for the clean domain, where core coverage is already high, the logifold IMM performs best.

| Dataset | $\mathcal{U}^{(0)}$ | $\mathcal{U}^{(1)}$ | All-ens | IMM |
|--|---------------------|---------------------|---------|---------------|
| $\mathcal{D}_{\text{clean}}, \tau = 1.4$ | 94.33% | 94.23% | N/A | N/A |
| $\mathcal{D}_{\text{weak}}, \tau = 0.96$ | 66.69% | 77.32% | 81.40% | 85.44% |
| $\mathcal{D}_{\text{strong}}, \tau = 0.02$ | 13.16% | 21.48% | 45.50% | 90.93% |
| $\mathcal{D}_{\text{union}}, \tau = 0.66$ | 58.06% | 64.34% | 74.62% | 87.48% |

(b) Total entropy H (Def. 3.2) on each domain at the selected τ . We observe a decrease in total entropy, which is an important signal of successful lifelong ensemble learning.

| Dataset | $\mathcal{U}^{(1)}$ | IMM |
|--|---------------------|--------------|
| $\mathcal{D}_{\text{weak}}, \tau = 0.96$ | $H = 0.6408$ | $H = 0.2876$ |
| $\mathcal{D}_{\text{strong}}, \tau = 0.02$ | $H = 1.9782$ | $H = 0.2054$ |
| $\mathcal{D}_{\text{union}}, \tau = 0.66$ | $H = 0.9638$ | $H = 0.2317$ |

tion set to ensure high core accuracy for $\mathcal{U}^{(1)}$ (see Fig. 1 in Appendix B).

On clean data, $\mathcal{C}_\tau(\mathcal{U}^{(1)})$ covers most samples, so we do not construct a second generation. On the other domains, the out-of-core region becomes non-negligible, and we train out-of-core specialists $\mathcal{U}^{(2)'}'$ and form IMM = $\mathcal{U}^{(1)} \cup \mathcal{U}^{(2)'}'$, a two-generation logifold (IMM: *Immunization Mechanism*).

The IMM aggregator is

$$\Gamma^{(2)}(\text{IMM}) := \mathbf{1}_{\mathcal{C}_\tau(\mathcal{U}^{(1)})} \Gamma^{(1)}(\mathcal{U}^{(1)}) + \mathbf{1}_{\mathcal{C}_\tau^c(\mathcal{U}^{(1)})} \Gamma^{(2)'}(\mathcal{U}^{(2)'}), \quad (9)$$

where $\Gamma^{(1)}$ and $\Gamma^{(2)'}'$ are probability averages on their respective ensembles. We compare overall accuracy P and total entropy H across $\Gamma^{(0)}$ (baseline $\mathcal{U}^{(0)}$), $\Gamma^{(1)}$ (first generation $\mathcal{U}^{(1)}$), and $\Gamma^{(2)}$ (IMM) in Table 2. We also report transfer-based AutoAttack results.

Remark. In Definition 4.2, the memory formation functional I is required to be non-decreasing. In our experiments, we use the total entropy H as a proxy for I , but H is expected to decrease as learning progresses. Thus, when reporting H we implicitly adopt a monotone reparameterization of memory formation. The distinction is a matter of directionality.

Table 2a shows that IMM improves overall accuracy on $\mathcal{D}_{\text{union}}$ (from 64.34% with $\mathcal{U}^{(1)}$ to 87.48%), and also yields the best performance on $\mathcal{D}_{\text{weak}}$ and $\mathcal{D}_{\text{strong}}$ among the com-

pared aggregation rules. Given changing environments, we observe that the inequality in lifelong ensemble learning $P(\Gamma^{(1)}) < P(\Gamma^{(2)})$ holds. Table 2b reports a consistent reduction in total entropy from $\mathcal{U}^{(1)}$ to IMM on non-clean environments.

Finally, we consider transfer-based AutoAttack at $\epsilon = 0.5$ and evaluate $\mathcal{U}^{(0)}$, $\mathcal{U}^{(1)}$ and IMM evolved on $\mathcal{D}_{\text{union}}$ with $\tau = 0.66$. The accuracy of $\mathcal{U}^{(0)}$, $\mathcal{U}^{(1)}$, IMM are 78.47%, 84.71% and 83.58% respectively. The result is comparable with $\mathcal{D}_{\text{weak}}$ shown in Table 2a, which suggests that the AutoAttack under consideration is slightly weaker than $\mathcal{D}_{\text{weak}}$ and hence $\mathcal{U}^{(1)}$ attains the highest overall accuracy. On the other hand, we observe that even in this case, IMM increases core coverage from 0.4581 ($\mathcal{U}^{(1)}$) to 0.7096 while improving high core accuracy from 95.87% ($\mathcal{U}^{(1)}$) to 97.04%.

6. Conclusion

We established two fundamental laws concerning work done and entropy for learning dynamics of models and ensembles. We formulated the notion of cores for ensembles, which utilizes the ensemble entropy as a label-free quantity of fuzziness and disagreement.

We constructed an immunized architecture IMM for detecting and adapting to polluted environments by adversarial perturbations. IMM consists of an immunized generation consisting of both models trained on clean data and models transferred to weakly perturbed data to detect effective adversarial samples, and a specialized generation that consists of models transferred to out-of-core samples. On CIFAR-10 under APGD-CE and surrogate-based AutoAttack, the resulting system IMM improves accuracy on mixed domains and yields particularly large gains under strong perturbations compared to naive averaging baselines.

More broadly, our approach suggests a principled way to grow modular ensembles over expanding domains by (i) identifying the core (trustworthy regions) via low ensemble entropy, (ii) transferring models to the complement of the core, and (iii) iterating this process to enlarge the core.

Impact Statement

This paper presents work whose goal is to advance the field of Machine Learning. There are many potential societal consequences of our work, none of which we feel must be specifically highlighted here.

References

Nested learning: The illusion of deep learning architecture. *Google Research*.

Andreas, J., Rohrbach, M., Darrell, T., and Klein, D. Neural module networks. In *2016 IEEE Conference on Computer Vision and Pattern Recognition, CVPR 2016, Las Vegas, NV, USA, June 27-30, 2016*, pp. 39–48. IEEE Computer Society, 2016. doi: 10.1109/CVPR.2016.12.

Anthony, M. and Bartlett, P. L. *Neural Network Learning: Theoretical Foundations*. Cambridge University Press, 2009. ISBN 978-0-521-11862-0.

Bai, Y., Anderson, B. G., and Sojoudi, S. Mixing classifiers to alleviate the accuracy-robustness trade-off. In Abate, A., Cannon, M., Margellos, K., and Papachristodoulou, A. (eds.), *Proceedings of the 6th Annual Learning for Dynamics and Control Conference*, volume 242 of *Proceedings of Machine Learning Research*, pp. 852–865. PMLR, 15–17 Jul 2024.

Baltrušaitis, T., Ahuja, C., and Morency, L.-P. Multimodal machine learning: A survey and taxonomy. *IEEE Transactions on Pattern Analysis and Machine Intelligence*, 41(2):423–443, 2019. doi: 10.1109/TPAMI.2018.2798607.

Bellman, R. E. *Dynamic Programming*. Princeton University Press, 2010. ISBN 9780691146683.

Ben-David, S., Blitzer, J., Crammer, K., Kulesza, A., Pereira, F. C., and Vaughan, J. W. A theory of learning from different domains. *Machine Learning*, 79:151–175, 2010.

Bengio, E., Bacon, P.-L., Pineau, J., and Precup, D. Conditional computation in neural networks for faster models. *ArXiv*, 2202.08906, 2015.

Carlini, N. and Wagner, D. Towards evaluation the robustness of neural networks. pp. 39–57, 2017.

Chen, J., Raghuram, J., Choi, J., Wu, X., Liang, Y., and Jha, S. Stratified adversarial robustness with rejection. In Krause, A., Brunskill, E., Cho, K., Engelhardt, B., Sabato, S., and Scarlett, J. (eds.), *Proceedings of the 40th International Conference on Machine Learning*, volume 202 of *Proceedings of Machine Learning Research*, pp. 4867–4894. PMLR, 23–29 Jul 2023. URL <https://proceedings.mlr.press/v202/chen23w.html>.

Choromańska, A., Henaff, M., Mathieu, M., Arous, G. B., and LeCun, Y. The loss surfaces of multilayer networks. In *International Conference on Artificial Intelligence and Statistics*, 2014.

Croce, F. and Hein, M. Reliable evaluation of adversarial robustness with an ensemble of diverse parameter-free attacks. In *ICML*, 2020.

Croce, F., Andriushchenko, M., Sehwag, V., Debenedetti, E., Flammarion, N., Chiang, M., Mittal, P., and Hein, M. Robustbench: a standardized adversarial robustness benchmark. In *Thirty-fifth Conference on Neural Information Processing Systems Datasets and Benchmarks Track*, 2021.

Depeweg, S., Hernández-Lobato, J. M., Doshi-Velez, F., and Udluft, S. Decomposition of uncertainty in bayesian deep learning for efficient and risk-sensitive learning. In *International Conference on Machine Learning*, 2017.

Fedus, W., Zoph, B., and Shazeer, N. Switch transformers: scaling to trillion parameter models with simple and efficient sparsity. *J. Mach. Learn. Res.*, 23(1), 2022. ISSN 1532-4435.

Ganin, Y., Ustinova, E., Ajakan, H., Germain, P., Larochelle, H., Laviolette, F., Marchand, M., and Lempitsky, V. Domain-adversarial training of neural networks. *J. Mach. Learn. Res.*, 17(1):2096–2030, 2016. ISSN 1532-4435.

Ge, R., Huang, F., Jin, C., and Yuan, Y. Escaping from saddle points — online stochastic gradient for tensor decomposition. In Grünwald, P., Hazan, E., and Kale, S. (eds.), *Proceedings of The 28th Conference on Learning Theory*, volume 40 of *Proceedings of Machine Learning Research*, pp. 797–842, Paris, France, 03–06 Jul 2015. PMLR.

Goodfellow, I. J., Shlens, J., and Szegedy, C. Explaining and harnessing adversarial examples. In Bengio, Y. and LeCun, Y. (eds.), *3rd International Conference on Learning Representations, ICLR 2015, San Diego, CA, USA, May 7-9, 2015, Conference Track Proceedings*, 2015.

Gulrajani, I. and Lopez-Paz, D. In search of lost domain generalization. *ArXiv*, abs/2007.01434, 2020.

Guo, C., Pleiss, G., Sun, Y., and Weinberger, K. Q. On calibration of modern neural networks. In Precup, D. and Teh, Y. W. (eds.), *Proceedings of the 34th International Conference on Machine Learning*, volume 70 of *Proceedings of Machine Learning Research*, pp. 1321–1330. PMLR, 06–11 Aug 2017. URL <https://proceedings.mlr.press/v70/guo17a.html>.

Guo, Y., Liu, M., Yang, T., and Rosing, T. Improved schemes for episodic memory-based lifelong learning. *ArXiv*, abs/1909.11763, 2019.

Haarnoja, T., Zhou, A., Abbeel, P., and Levine, S. Soft actor-critic: Off-policy maximum entropy deep reinforcement learning with a stochastic actor. *Proceedings of Machine Learning Research*, 2018.

He, K., Zhang, X., Ren, S., and Sun, J. Deep residual learning for image recognition. *2016 IEEE Conference on Computer Vision and Pattern Recognition (CVPR)*, pp. 770–778, 2015.

Hendrycks, D. and Gimpel, K. A baseline for detecting misclassified and out-of-distribution examples in neural networks. In *5th International Conference on Learning Representations, ICLR 2017, Toulon, France, April 24-26, 2017, Conference Track Proceedings*, 2017. URL <https://openreview.net/forum?id=Hkg4TI9x1>.

Jacobs, R. A., Jordan, M. I., Nowlan, S. J., and Hinton, G. E. Adaptive mixtures of local experts. *Neural Computation*, 3(1):79–87, 03 1991. ISSN 0899-7667. doi: 10.1162/neco.1991.3.1.79.

Jacot, A., Gabriel, F., and Hongler, C. Neural tangent kernel: convergence and generalization in neural networks. In *Proceedings of the 32nd International Conference on Neural Information Processing Systems, NIPS’18*, pp. 8580–8589, Red Hook, NY, USA, 2018. Curran Associates Inc.

Jung, I. and Lau, S.-C. Logifold: A geometrical foundation of ensemble machine learning. In *2024 4th International Conference on Electrical, Computer, Communications and Mechatronics Engineering (ICECCME)*, pp. 1–6. Male, Maldives, 2024.

Jung, I. and Lau, S.-C. A logifold structure on measure space. *Axioms*, 14(8), 2025.

Khalil, H. K. *Nonlinear Systems*. Cambridge University Press, 3rd edition, 2011. ISBN 978-0130673893.

Kingma, D. P. and Ba, J. Adam: A method for stochastic optimization. In Bengio, Y. and LeCun, Y. (eds.), *3rd International Conference on Learning Representations, ICLR 2015, San Diego, CA, USA, May 7-9, 2015, Conference Track Proceedings*, 2015.

Kirkpatrick, J., Pascanu, R., Rabinowitz, N., Veness, J., Desjardins, G., Rusu, A. A., Milan, K., Quan, J., Ramalho, T., Grabska-Barwinska, A., Hassabis, D., Clopath, C., Kumaran, D., and Hadsell, R. Overcoming catastrophic forgetting in neural networks. *Proceedings of the National Academy of Sciences*, 114(13):3521–3526, 2017. doi: 10.1073/pnas.1611835114.

Krizhevsky, A. Learning multiple layers of features from tiny images, 2009.

Laidlaw, C. and Feizi, S. Playing it safe: Adversarial robustness with an abstain option. *CoRR*, abs/1911.11253, 2019. URL <http://arxiv.org/abs/1911.11253>.

Lakshminarayanan, B., Pritzel, A., and Blundell, C. Simple and scalable predictive uncertainty estimation using deep ensembles. In *Proceedings of the 31st International Conference on Neural Information Processing Systems, NIPS’17*, pp. 6405–6416, Red Hook, NY, USA, 2017. Curran Associates Inc. ISBN 9781510860964.

Lee, K., Lee, K., Lee, H., and Shin, J. A simple unified framework for detecting out-of-distribution samples and adversarial attacks. In *Proceedings of the 32nd International Conference on Neural Information Processing Systems*, pp. 7167–7177, 2018.

Lepikhin, D., Lee, H., Xu, Y., Chen, D., Firat, O., Huang, Y., Krikun, M., Shazeer, N., and Chen, Z. Gshard: Scaling giant models with conditional computation and automatic sharding. *ICLR*, 2020.

Liu, S. and Deng, W. Very deep convolutional neural network based image classification using small training sample size. In *2015 3rd IAPR Asian Conference on Pattern Recognition (ACPR)*, pp. 730–734, 2015. doi: 10.1109/ACPR.2015.7486599.

Mandt, S., Hoffman, M. D., and Blei, D. M. Stochastic gradient descent as approximate bayesian inference. *J. Mach. Learn. Res.*, 18(1):4873–4907, 2017.

McCloskey, M. and Cohen, N. J. Catastrophic interference in connectionist networks: The sequential learning problem. volume 24 of *Psychology of Learning and Motivation*, pp. 109–165. Academic Press, 1989. doi: [https://doi.org/10.1016/S0079-7421\(08\)60536-8](https://doi.org/10.1016/S0079-7421(08)60536-8).

Mei, S., Montanari, A., and Nguyen, P.-M. A mean field view of the landscape of two-layer neural networks. *Proceedings of the National Academy of Sciences*, 115(33): E7665–E7671, 2018. doi: 10.1073/pnas.1806579115.

Minsky, M. *The Society of Mind*. New York: Simon & Schuster, 1986. ISBN 0-671-60740-5.

Mnih, V., Kavukcuoglu, K., Silver, D., Rusu, A. A., Veness, J., Bellemare, M. G., Graves, A., Riedmiller, M. A., Fidjeland, A. K., Ostrovski, G., Petersen, S., Beattie, C., Sadik, A., Antonoglou, I., King, H., Kumaran, D., Wierstra, D., Legg, S., and Hassabis, D. Human-level control through deep reinforcement learning. *Nature*, 518:529–533, 2015.

Muandet, K., Balduzzi, D., and Scholkopf, B. Domain generalization via invariant feature representation. In *International Conference on Machine Learning*, 2013.

Ngiam, J., Khosla, A., Kim, M., Nam, J., Lee, H., and Ng, A. Multimodal deep learning. In *International Conference on Machine Learning*, 2011.

Ovadia, Y., Fertig, E., Ren, J., Nado, Z., Sculley, D., Nowozin, S., Dillon, J. V., Lakshminarayanan, B., and Snoek, J. *Can you trust your model's uncertainty? evaluating predictive uncertainty under dataset shift*. Curran Associates Inc., Red Hook, NY, USA, 2019.

Pang, T., Zhang, H., He, D., Dong, Y., Su, H., Chen, W., Zhu, J., and Liu, T.-Y. Two coupled rejection metrics can tell adversarial examples apart. *2022 IEEE/CVF Conference on Computer Vision and Pattern Recognition (CVPR)*, pp. 15202–15212, 2022. URL <https://api.semanticscholar.org/CorpusID:244955010>.

Parisi, G. I., Kemker, R., Part, J. L., Kanan, C., and Wermter, S. Continual lifelong learning with neural networks: A review. *Neural Networks*, 113:54–71, 2019. ISSN 0893-6080. doi: <https://doi.org/10.1016/j.neunet.2019.01.012>.

Puterman, M. L. *Markov Decision Processes: Discrete Stochastic Dynamic Programming*. John Wiley & Sons, Inc., 1994. ISBN 9780470316887.

Radford, A., Kim, J. W., Hallacy, C., Ramesh, A., Goh, G., Agarwal, S., Sastry, G., Askell, A., Mishkin, P., Clark, J., Krueger, G., and Sutskever, I. Learning transferable visual models from natural language supervision. In *International Conference on Machine Learning*, 2021.

Schulman, J., Levine, S., Abbeel, P., Jordan, M., and Moritz, P. Trust region policy optimization. In Bach, F. and Blei, D. (eds.), *Proceedings of the 32nd International Conference on Machine Learning*, volume 37 of *Proceedings of Machine Learning Research*, pp. 1889–1897, Lille, France, 07–09 Jul 2015. PMLR.

Schulman, J., Wolski, F., Dhariwal, P., Radford, A., and Klimov, O. Proximal policy optimization algorithms. *ArXiv*, abs/1707.06347, 2017.

Schweigofer, K., Aichberger, L., Ielanskyi, M., and Hochreiter, S. On information-theoretic measures of predictive uncertainty. In *The 41st Conference on Uncertainty in Artificial Intelligence*, 2025.

Shannon, C. E. A mathematical theory of communication. *The Bell System Technical Journal*, 27:379–423, 623–656, 1948.

Shazeer, N., Mirhoseini, A., Maziarz, K., Davis, A., Le, Q. V., Hinton, G. E., and Dean, J. Outrageously large neural networks: The sparsely-gated mixture-of-experts layer. *ICLR*, 2017.

Soudry, D., Hoffer, E., Nacson, M. S., Gunasekar, S., and Srebro, N. The implicit bias of gradient descent on separable data. *J. Mach. Learn. Res.*, 19:1–57, 2018.

Srivastava, N. and Salakhutdinov, R. R. Multimodal learning with deep boltzmann machines. In Pereira, F., Burges, C., Bottou, L., and Weinberger, K. (eds.), *Advances in Neural Information Processing Systems*, volume 25. Curran Associates, Inc., 2012.

Sutton, R. and Barto, A. Reinforcement learning: An introduction. *IEEE Transactions on Neural Networks*, 9(5): 1054–1054, 1998. doi: 10.1109/TNN.1998.712192.

Sutton, R. S., McAllester, D., Singh, S., and Mansour, Y. Policy gradient methods for reinforcement learning with function approximation. In *Proceedings of the 13th International Conference on Neural Information Processing Systems*, NIPS'99, pp. 1057–1063, Cambridge, MA, USA, 1999. MIT Press.

Thrun, S. *Lifelong Learning Algorithms*, pp. 181–209. Springer US, Boston, MA, 1998. ISBN 978-1-4615-5529-2. doi: 10.1007/978-1-4615-5529-2_8.

Tramer, F., Carlini, N., Brendel, W., and Madry, A. On adaptive attacks to adversarial example defenses. In Larochelle, H., Ranzato, M., Hadsell, R., Balcan, M., and Lin, H. (eds.), *Advances in Neural Information Processing Systems*, volume 33, pp. 1633–1645. Curran Associates, Inc., 2020.

Tsipras, D., Santurkar, S., Engstrom, L., Turner, A., and Madry, A. Robustness may be at odds with accuracy. In *International Conference on Learning Representations*, 2018.

van de Ven, G. M., Soures, N., and Kudithipudi, D. *Continual learning and catastrophic forgetting*, pp. 153–168. Elsevier, 2025. ISBN 9780443157554. doi: 10.1016/b978-0-443-15754-7.00073-0.

Wang, X. and Yiu, S. M. Classification with rejection: scaling generative classifiers with supervised deep infomax. In *Proceedings of the Twenty-Ninth International Joint Conference on Artificial Intelligence*, IJCAI'20, 2021. ISBN 9780999241165.

Williams, R. J. Simple statistical gradient-following algorithms for connectionist reinforcement learning. *Mach. Learn.*, 8(3–4):229–256, 1992. ISSN 0885-6125. doi: 10.1007/BF00992696.

Zhang, H., Yu, Y., Jiao, J., Xing, E. P., Ghaoui, L. E., and Jordan, M. I. Theoretically principled trade-off between robustness and accuracy. In *International Conference on Machine Learning*, 2019.

Zoph, B., Bello, I., Kumar, S., Du, N., Huang, Y., Dean, J., Shazeer, N., and Fedus, W. St-moe: Designing stable and transferable sparse expert models. volume 2202.08906, 2022.

A. Proofs

A.1. Proof of Proposition 2.4

Proof.

$$-(\text{grad } H)|_y \cdot y' = -h(y', y) + \sum_a y'_a$$

by direct calculation. for y' being tangent to Δ , the second term vanishes. Thus the integrand on the left hand side becomes

$$h(\mathcal{T}(x) - F(x), F(x)) = h(\mathcal{T}(x), F(x)) - H(F(x))$$

where $F = f \circ \Phi$. Integration over $\text{Dom}(\Phi)$ gives the equality. \square

A.2. Proof of Theorem 3.5

Proof. Note that each term of $H(\mathcal{U})$ in Definition 3.2 is non-negative. Thus, $H(\mathcal{U}) = 0$ if and only if $\mu(X - \bigcup_{l=1}^K \text{Dom}(\Phi_l)) = 0$ and $H((\Phi_l, f_l), (\Phi_r, f_r)) = 0$ for every l, r . $H((\Phi_l, f_l), (\Phi_r, f_r))$ is an integral of a non-negative function. By monotone convergence theorem in measure theory, the integral is zero if and only if the non-negative functions $-f_{l,a}(\Phi_l(x)) \log_t f_{r,a}(\Phi_r(x)) = 0$ almost everywhere. For $l = r$, this happens if and only if $f_{l,a}(\Phi_l(x)) \in \{0, 1\}$ for $x \in S'_l$ where $\mu(\text{Dom}(\Phi_l) - S'_l) = 0$; since the image of f_l lies in the simplex $\Delta(T_l)$, $f_{l,a}(\Phi_l(x)) = 1$ for exactly one value of $a \in T_l$ and 0 otherwise; hence it gives a function F_l on S'_l . For $l \neq r$, this happens if and only if $f_{l,a}(\Phi_l(x)) = f_{r,a}(\Phi_r(x))$ for $x \in S'_{lr}$ where $\mu(\text{Dom}(\Phi_l) \cap \text{Dom}(\Phi_r) - S') = 0$. In this situation, for each $x \in X$, we define $F(x) = F_1(x)$ if $x \in S'_1$, $F(x) = F_2(x)$ if $x \in S'_2 - S'_1$, $F(x) = F_3(x)$ if $x \in S'_3 - S'_2 - S'_1$ and so on; $F(x)$ is assigned to be a fixed element in Y if $x \in X - \bigcup_i S'_i$ which is a measure zero set. By construction, $F|_{\text{Dom}(\Phi_l)} = f_l \circ \Phi_l$ almost everywhere for every $l = 1, \dots, K$. \square

A.3. Proof of Proposition 3.8

Proof. First, we have $C_p(\mathcal{U}) \subset \bigcup_l \text{Dom}(\Phi_l)$ since $H_x(\mathcal{U}) < \log_{|Y|} 2 < K^2$ for all $x \in C_p(\mathcal{U})$. Moreover, since every term in (2) is non-negative, $H_x(\mathcal{U}) < \log_{|Y|} 2$ implies that every term $H_x((\Phi_l, f_l), (\Phi_r, f_r)) = \sum_{a=1}^t -F_{l,a}(x) \log_t F_{r,a}(x) < \log_{|Y|} 2$ where $F_i = f_i \circ \Phi_i$ and $t = |T_l \cup T_r|$. Let's consider the terms for $l = r$. The subset $\{y \in \Delta(T_l) : \sum_{a=1}^t -y_{a,a} \log_t y_{a,a} < \log_{|Y|} 2\}$ has t connected components; for all y lying in the a -th component, $y_{a,a}$ is the unique maximum among the entries of y . This proves the first statement for the uniqueness of $a \in T_l$. Now consider $y_l = F_l(x)$ and $y_r = F_r(x)$ for $x \in C_p(\mathcal{U})$ and $\text{Dom}(\Phi_l) \cap \text{Dom}(\Phi_r) \ni x$. For every $a \in T$, it needs to satisfy the inequalities

$$\begin{aligned} -(y_{l,a} \log_t y_{r,a} + y_{r,a} \log_t y_{l,a}) &< 2/|Y| < 2/t; \\ -(y_{l,a} \log_t y_{r,a} + y_{r,a} \log_t y_{l,a}) &< \log_{|Y|} \frac{3}{2} < \log_t \frac{3}{2} \end{aligned}$$

where the second inequality reduces to

$$-(y_{l,a} \log y_{r,a} + y_{r,a} \log y_{l,a}) < \log \frac{3}{2}.$$

For each a , the subset of all $(y_{l,a}, y_{r,a}) \in [0, 1] \times [0, 1]$ that satisfies the inequalities consists of two components that are subsets of $\{\text{both } y_{l,a} \text{ and } y_{r,a} < \frac{1}{|Y|}\}$ (using the first inequality) and $\{\text{both } y_{l,a} \text{ and } y_{r,a} > \frac{1}{2}\}$ (using the second inequality) respectively. For those indices a that are not argmax of y_l , we have $y_{l,a} < 1/2$ which implies $y_{r,a} < \frac{1}{|Y|} < \frac{1}{|T_r|}$. Let a_0 be the argmax of y_l . Then $y_{r,a_0} = 1 - \sum_{a \neq a_0} y_{r,a} > \frac{1}{|T_r|} > \frac{1}{|Y|}$, and hence (y_{l,a_0}, y_{r,a_0}) lies in the second component which implies a_0 is also the argmax of y_r . Thus y_l and y_r have the same argmax a_0 . Thus models give the same response (after taking argmax) in the intersections, and hence we have a well-defined function $F : C_p(\mathcal{U}) \rightarrow Y$. \square

A.4. Proof of Theorem 3.11

Proof. By (5) and Theorem 2.6, the entropy of each model in an ensemble that survives in the limit has entropy limiting to zero. Thus, it suffices to consider the cross entropy of any two different models in an ensemble. Since each domain and target stabilize, we may assume that their domains and targets are independent of the step i . Let's denote their domains by

$D_l \subset X$, targets by $T_l \subset Y$ and the model functions by $F_l^{(i)} = (F_{l,a}^{(i)} : a \in T_l)$ respectively for $l = 1, 2$. Take any $\epsilon > 0$ and $n > 0$. For i large enough, as in the proof of Theorem 2.6, we have a subset $S_l \subset D_l$ with $\mu(D_l - S_l) < \epsilon$ such that for all $x \in S$,

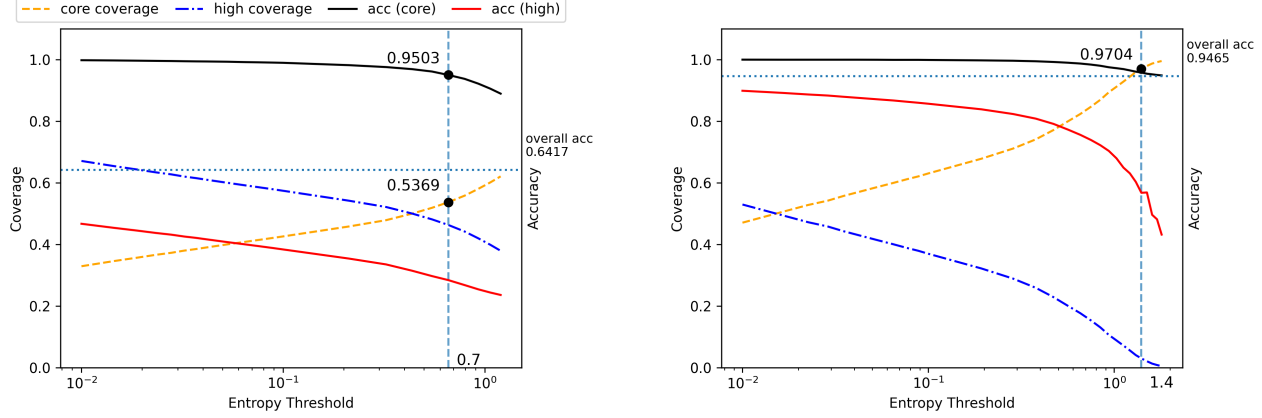
$$-\log_{t_l} F_{l,\mathcal{T}(x)}^{(i)}(x) < \frac{1}{n},$$

that is, $F_{l,\mathcal{T}(x)}^{(i)}(x) > 1/(t_l)^{1/n}$ (meaning that it can be made arbitrarily close to 1). The pointwise cross entropy between the two is

$$-F_{1,\mathcal{T}(x)}^{(i)}(x) \log_{t_2} F_{2,\mathcal{T}(x)}^{(i)}(x) - \sum_{a \neq \mathcal{T}} F_{1,a}^{(i)}(x) \log_{t_2} F_{2,a}^{(i)}(x).$$

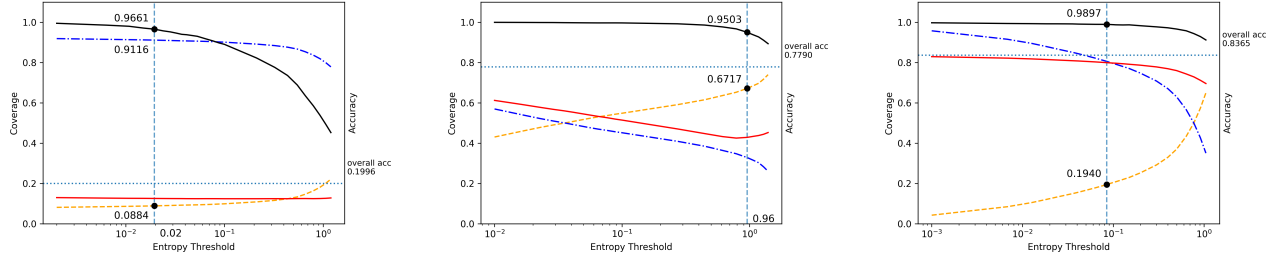
Let $x \in S_1 \cap S_2$. For the first term, $-\log_{t_2} F_{2,\mathcal{T}(x)}^{(i)}(x) < 1/n$ and $F_{1,\mathcal{T}(x)}^{(i)}(x) < 1$, implying that the first term $< 1/n$. For each summand of the second term, $F_{1,a}^{(i)}(x) < 1 - 1/(t_l)^{1/n} < 1 - 1/|Y|^{1/n} < \epsilon/|Y|$ by taking n large. Thus, the pointwise entropy for $x \in S_1 \cap S_2$ can be made arbitrarily small. Moreover, $\mu(D_1 \cap D_2 - S_1 \cap S_2) < \epsilon$. Thus, the cross entropy between any two models in $\mathcal{U}^{(i)}$ can be made arbitrarily small for i sufficiently large. Thus, $H(\mathcal{U}^{(i)})$ defined by (3) can be made arbitrarily small. \square

B. Graphs of Core Coverage and Accuracy under Entropy thresholding.



(a) $\mathcal{D}_{\text{union, val}}$. At $\tau = 0.7$ the core accuracy is greater than 95%.

(b) $\mathcal{D}_{\text{clean, val}}$. At $\tau = 1.4$, the core coverage is 0.9704.



(c) $\mathcal{D}_{\text{strong, val}}$, $\tau = 0.02$

(d) $\mathcal{D}_{\text{weak}}$, $\tau = 0.96$

(e) AutoAttack ($\epsilon = 0.5$). The vertical line is at $\tau = 0.1$. It shows that the immunized generation detects transfer-based adversarial samples reliably.

Figure 1. Accuracy and coverage under entropy thresholding across domains. Solid curves show accuracies on \mathcal{C}_τ (black) and \mathcal{C}_τ^c (red). Dashed curves show coverages of \mathcal{C}_τ (orange) and \mathcal{C}_τ^c (blue). The vertical dashed line marks the selected τ for a validation accuracy target of 95.25%. Across domains, decreasing τ monotonically decreases core coverage while increasing core accuracy. Moreover, the core accuracy is consistently above the overall accuracy, whereas the out-of-core accuracy is consistently below it.